

Conformational study of a sugar nitroxyl free radical

Jean M. J. Tronchet*, Alessandra Ricca, Françoise Barbalat-Rey,

Institute of Pharmaceutical Chemistry, University of Geneva, Sciences II, CH-1211 Geneva 4 (Switzerland)

and Michel Geoffroy

Department of Physical Chemistry, University of Geneva, Sciences II, CH-1211 Geneva 4 (Switzerland)

(Received August 10th, 1990; accepted for publication, October 23rd, 1990)

ABSTRACT

Ethyl 2,3-dideoxy-2-isopropylamino- α -D-arabino-hexopyranoside *N*-oxyl and its 2'-*d* analogue have been studied by variable-temperature e.s.r. spectroscopy. At low temperature, two frozen conformers (**5**, $a_{H-2} = 15.5$ G; and **6**, $a_{H-2} = 1.8$ G) were found. Semi-empirical quantum mechanics and molecular mechanics, using specially developed parameters for hydroxylamines and nitroxyls, helped to assign an almost eclipsed geometry (O–N–C–2–C–1 $\sim 10^\circ$) to **5** and a compromise between a staggered and the nearest eclipsed conformation (O–N–C–2–C–1 $\sim 80^\circ$) to **6**.

INTRODUCTION

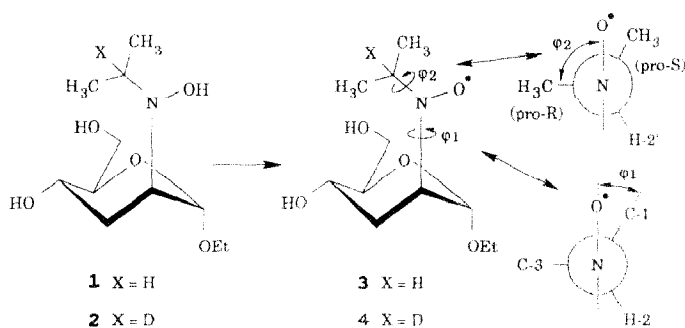
Deoxyhydroxyamino sugars can be prepared readily by several pathways^{1–3}. The major interest in these compounds resides in the closeness of their structures to their sugar models and their spontaneous oxidation to nitroxyl free radicals, the e.s.r. spectra of which provide information on structure that cannot be obtained by other spectroscopic methods. The imino-*N*-oxyl group is an almost perfect model of the carbonyl group and, when it replaces the oxygen bridge of a blocked disaccharide⁴, it gives information on the steric demand of the two sugar moieties. We have shown⁵ that an axial nitroxyl is free to rotate, and, at room temperature, there are different conformations. We now report on these conformations.

RESULTS AND DISCUSSION

Ethyl 2,3-dideoxy-2-(*N*-hydroxy-*N*-isopropylamino)- α -D-arabino-hexopyranoside⁶ (**1**) and its 2'-deuterio analogue **2** spontaneously oxidised to the corresponding nitroxyl derivatives⁶, **3** and **4**, respectively. Glycoside **1** exists in the ⁴C₁ conformation in the solid state and in solution.⁶ The same conformation is assumed for **3** and **4**.

E.s.r. spectroscopy. — The e.s.r. spectra of **3** and **4** were measured at temperatures in the range -50° to $+120^\circ$ for solutions in 1,2-dimethoxyethane and diglyme (Table I). Comparison of the spectra allowed the assignment of a_{H-2} and $a_{H-2'}$. Eventual long-range couplings were not resolved and are included in the line-width (I).

* Author for correspondence.



At $<0^\circ$, two frozen conformers **5** and **6** were found in the ratio $\sim 4:5$. The hyperfine coupling constants were extracted best from the spectra of a solution of **3** in dimethoxyethane at -45° . From the relationship⁴ [$a_{\text{H}}/\text{G} = (25 \pm 1)\cos^2\theta$], adapted from that of Rassat and co-workers⁷ ($a_{\text{H}}/\text{G} = 26\cos^2\theta$) where θ is the dihedral angle between a vicinal C-H bond and the p_z orbital of the nitrogen atom, the θ values that corresponded to $a_{\text{H-2}}$ were $38 \pm 1.5^\circ$ for **5** and $74.4 \pm 0.3^\circ$ for **6**. This finding gives four possible values of the dihedral angle φ_1 (C-1-C-2-N-O) for **5** (**5a-d**) and the same number for **6** (**6a-d**). None of these conformers is perfectly eclipsed or staggered and they are rotated by $12 \pm 4^\circ$ from a pure conformation. This result is reminiscent of the fact that, when a double bond is assumed to eclipse a vicinal group, a dihedral angle of $\sim 10^\circ$ is often found by X-ray diffraction (see, for example, ref. 8). When the temperature was increased, coalescence was observed and the signals then sharpened to give the time-averaged spectra. The time-averaged value of $a_{\text{H-2}}$ was lower than the mean value of the frozen conformers **5** and **6**, and decreased with increase in temperature; the ratio [**5**]/[**6**] was 2:3 at 75° for a solution in 1,2-dimethoxyethane.

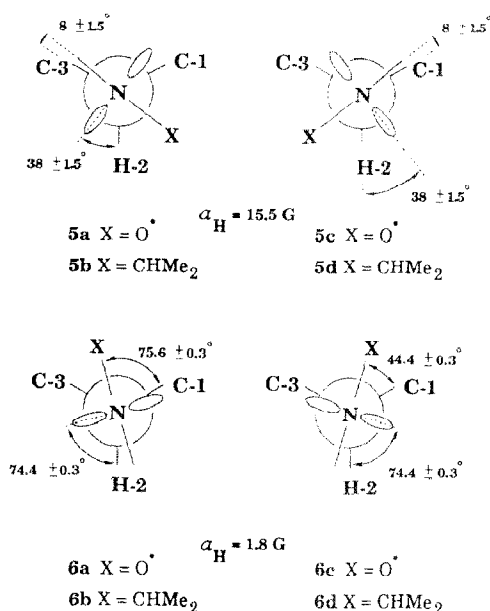


TABLE I

E.s.r. data for nitroxyls 3 and 4^a

Temp. (°)		In 1,2-dimethoxyethane										In diglyme									
		3					4					3					4				
		a_{H-2}	a_{H-2}	Γ	a_{H-2}	a_{D-2}	Γ	a_{H-2}	a_{H-2}	a_{D-2}	Γ	a_{H-2}	a_{H-2}	a_{D-2}	Γ	a_{H-2}	a_{H-2}	a_{D-2}	Γ		
5	6	5	6	5	6	5	6	5	6	5	6	5	6	5	6	5	6	5	6		
-50						15.5				0.5	1	2									
-45																					
-20																14.7		0.5	1.2		
-10																					
0						14															
10																					
30																					
45																					
50																					
60																					
75																					
80																					
120																					

^a $g = 2.0059$, $a_N = 14.8 \pm 0.2$ G; a_H , a_D , and Γ in G.

On the other hand, the time-averaged value of $a_{\text{H-2}}$ was much larger than either of those of **5** and **6**, and increased with the temperature to 4.8 G for a solution in diglyme at 120°, which represents the value encountered in freely rotating *N*-isopropylnitroxyl derivatives like 6-deoxy-6-isopropylamino-1,2:5,6-di-*O*-isopropylidene- α -D-galactopyranose *N*-oxyl¹. This behaviour on increasing the temperature implies a large entropy factor that favours **6**, which could be explained if **6** corresponded to a mixture of conformers that had the same $a_{\text{H-2}}$ value, or to a larger entropy content related to φ_2 . The latter hypothesis is favoured (see below).

The fact that $a_{\text{H-2}}$ and $a_{\text{H-2'}}$ were neither totally dependent nor independent made the determination of the energy barrier between **5** and **6** impossible by classical ways. In order to estimate the value of this barrier, the spectrum of **4** was used, thus replacing the $a_{\text{H-2}}$ coupling by a line broadening due to the hyperfine coupling with the deuterium atom. For a solution of **4** in diglyme, the coalescence temperature was 10° with a distance between homologous signals (δ_{H0}) at low temperature [$k_{\text{exchange}} (\text{s}^{-1}) \geq 0$] of 7.3 G. Using the Gutowski–Holm approximation⁹, the estimated rate constant k_{283} was $14.4 \times 10^8 \text{ s}^{-1}$ and the Gibbs free energy of activation from Eyring's equation¹⁰ was $\sim 4.7 \text{ kcal.mol}^{-1}$.

Quantum mechanics. – Starting with the crystal geometry of **1**, the hydrogen atom of the *N*-hydroxy group was removed under QUANTA^{*} and the new structure was submitted to the semi-empirical packages AMPAC¹¹ (RHF) and SCAMP¹² (UHF PULAY), using the AM1 Hamiltonian¹³. As AMPAC and MOPAC are known¹⁴ to exaggerate the bend of *sp*² nitrogen atoms, for example in amides, a constraint was established to ensure the flatness of the nitroxyl group. The dihedral angle φ_1 was varied from 0 to 350° in increments of 10° and, for each conformer, the geometry was fully optimised in the PRECISE mode, except for the incremented φ_1 and the C-2'-N-C-2-C-1 dihedral angle which was fixed by reference. The computing time necessary for each step along the reaction co-ordinate was in the range 6–25 h, which made impracticable a second incremental rotation about φ_2 . Consequently, the minimisation of the geometry led to a good, but not necessarily the best, value of φ_2 , and no provision was made to jump out of a possible local minimum. This situation was apparent from the fact that, in the RHF mode, the heats of formation obtained for a given value of φ_1 were slightly dependent on the starting geometry. In order to ensure the best possible consistency throughout the computation, the starting point was the φ_1 value (-37°) found in the crystal of **1**, the computation proceeded continuously from -30 to $+350^\circ$, and the results related to the negative φ_1 values were discarded. The heats of formation were then plotted against φ_1 (Fig. 1). In the RHF mode (Fig. 1, curve I), there were three broad minima (A–C) that corresponded to φ_1 10–20°, 90–100°, and 220–230°, respectively. The values of the heats of formation obtained from the UHF computations (Fig. 1, curve II) were lower than those obtained using RHF, but the overall shapes of the curves were almost identical except in the range 0–100°. The relatively low maxima do not represent true energy barriers but the less stable amongst the minimised conformers.

* A Trademark of Polygen Corporation.

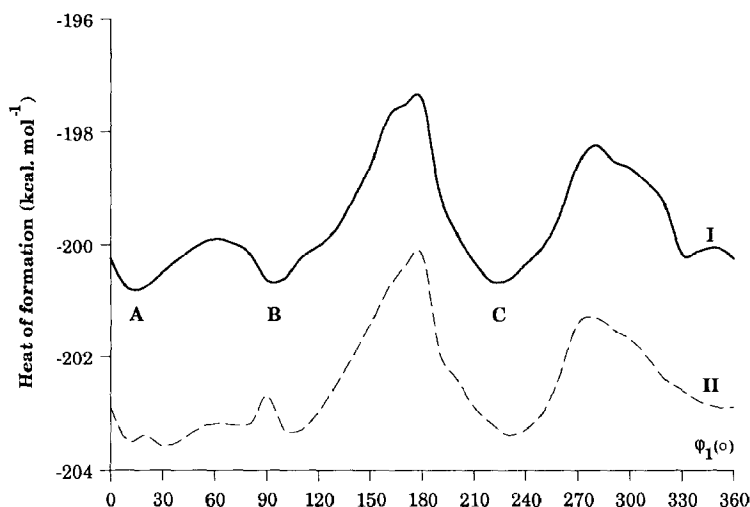


Fig. 1. Heat of formation of **1** (AM1 Hamiltonian) versus ϕ_1 : curve I computed by AMPAC (RHF), and curve II by SCAMP (UHF).

Molecular mechanics. — For this type of conformational analysis where two dihedral angles are involved principally, molecular mechanics are more adequate than quantum mechanics, mostly in terms of computational time. Molecular mechanics strongly depend on the quality of the relevant parameters and, as no parameters existed for hydroxylamines and nitroxyls, they were developed in CHARMM¹⁶. The following new types of atom were created (Table II): NHY (NROH), HHY (NHOR), OHY (NROH), NZ (NO[•]), and OZ (NO[•]). In the general CHARMM energy function¹⁵,

$$E = E_b + E_\theta + E_\phi + E_w + E_{vdw} + E_{cl} + E_{hb} + E_{er} + E_{e\phi},$$

where the last two terms represent constraints, only the bond potential (E_b), the bond-angle potential (E_θ), the torsion potential (E_ϕ), the improper torsion potential (E_w), and the van der Waals term E_{vdw} had to be parametrised explicitly for the new types of atom. For the E_{cl} term, the shifted dielectric mode and an ϵ_0 value of 1.0 were used, whereas for the E_{vdw} term, the shifted van der Waals option was chosen. Hydrogen bonds, unlikely in this situation, were not taken into account.

For the parametrisation, the classical strategy^{15,16} was used. The force constants of the internal energy terms were obtained by fitting to experimental vibrational data¹⁷. Other parameters were deduced from *ab initio* calculations¹⁸ or from X-ray diffraction data of sugar hydroxylamines^{1,6}, some by analogy with the parent compounds. Whenever possible, particularly for hydroxylamines, the parameters were fitted to X-ray diffraction data. All the parameters are collected in Table II.

The conformational search was performed with QUANTA and CHARMM, the primary rotation being ϕ_1 (increments of 10°); for each value of ϕ_1 , a 360° rotation of ϕ_2 (increments of 10°) was performed. For each set of ϕ_1 and ϕ_2 values, the molecule was relaxed using the adopted basis Newton–Raphson algorithm (up to 500 steps). The

TABLE II

Parameters introduced in the CHARMM force field for hydroxylamines and nitroxyls

Atom types													
At	Polarisability	ϵ_a^a	$1/2 \sigma_a^b$										
NHY	1.10	-0.2384	1.600										
HHY	0.044	-0.0498	0.800										
NZ	1.10	-0.2384	1.600										
OHY	0.84	-0.1591	1.600										
OZ	0.84	-0.1591	1.600										
Bonds													
At1	At2	k_b^b	r_0^b	At1	At2	k_b^c	r_0^c						
NZ	OZ	508.0	1.27	NHY	C	320.0	1.43						
NZ	CH3E	208.0	1.46	OHY	H	525.0	0.96						
NZ	CH1E	208.0	1.46	C6R	SO2	226.0	1.71						
NZ	CT	208.0	1.46 ^d	SO2	NT	320.0	1.693						
NHY	OHY	240.0	1.43	SO2	OC	528.0	1.50						
NHY	CH3E	270.0	1.46	OHY	CH3E	340.0	1.43						
NHY	CH1E	280.0	1.47	OHY	CH2E	340.0	1.43						
NHY	CH2E	280.0	1.48	OHY	CH1E	340.0	1.43						
NHY	CT	270.0	1.46	OHY	C	375.0	1.35						
NHY	C6R	320.0	1.425	OHY	CT	340.0	1.43 ^e						
NHY	HHY	436.0	1.01										
Torsional angles													
At1	At2	At3	At4	k_θ^g	n	δ^f	At1	At2	At3	At4	k_θ^g	n	δ^f
X	CH1E	NZ	X	1.4	3	0.0	X	CT	NHY	X	0.6	3	0.0
X	CT	NZ	X	1.4	3	0.0 ^d	X	C6R	NHY	X	1.0	2	180.0
X	NHY	OHY	X	6.0	12	0.0	X	OHY	C	X	1.0	2	180.0
X	NHY	C	X	4.0	2	180.0	X	OHY	CH2E	X	0.4	3	0.0
X	CH1E	NHY	X	0.5	3	0.0	X	OHY	CH1E	X	0.4	3	0.0
X	CH2E	NHY	X	0.2	3	0.0	X	OHY	CT	X	0.4	3	0.0 ^d
Improper torsions													
At1	At2	At3	At4	k_ω^e		w_0^i	At1	At2	At3	At4	k_ω^e		w_0^i
NZ	OZ	CH3E	CH3E	2.0	0	0.0	NHY	C6R	C6R	C6R	90.0	0	0.0
NZ	OZ	CH1E	CH1E	2.0	0	0.0	NHY	OHY	HHY	CH3E	0.0	0	0.0
NZ	OZ	CT	CT	2.0	0	0.0 ^d	NHY	OHY	HHY	CH1E	0.0	0	0.0
NZ	CT	CT	OZ	2.0	0	0.0	NHY	OHY	HHY	CT	0.0	0	0.0 ^f
NHY	OHY	CH3E	CH3E	0.0	0	0.0	NHY	CH1E	C	O	90.0	0	0.0
NHY	OHY	CH1E	CH1E	0.0	0	0.0	NHY	CT	C	O	90.0	0	0.0 ^e
NHY	OHY	CH2E	CH1E	0.0	0	0.0	NHY	CH1E	C	OHY	0.2	0	0.0
NHY	OHY	CT	CH2E	0.0	0	0.0	NHY	CT	C	OHY	0.2	0	0.0 ^e
NHY	OHY	CT	CT	0.0	0	0.0 ^f	C	NHY	CH3E	OHY	90.0	0	0.0
NHY	OHY	C6R	C6R	90.0	0	0.0	C	NHY	CT	OHY	90.0	0	0.0 ^e
NHY	OHY	CH1E	C6R	0.2	0	0.0	X	OHY	O	X	90.0	0	0.0
NHY	OHY	CT	C6R	0.2	0	0.0	C	OS	O	CH3E	90.0	0	0.0

Bond angles

<i>At1</i>	<i>At2</i>	<i>At3</i>	k_9^e	θ_p^f	<i>At1</i>	<i>At2</i>	<i>At3</i>	k_9^e	θ_p^f
CH3E	NZ	OZ	40.0	120.0	NHY	C6R	HA	70.0	120.0
CH1E	NZ	OZ	40.0	120.0	NHY	OHY	H	60.0	109.47
CT	NZ	OZ	40.0	120.0 ^d	NHY	C	O	84.0	121.0
CH3E	NZ	CH3E	35.0	120.0	CH3E	NHY	HHY	60.0	107.0
CH1E	NZ	CH1E	35.0	120.0	CH1E	NHY	HHY	60.0	107.0
CT	NZ	CT	35.0	120.0 ^d	CT	NHY	HHY	60.0	107.0 ^d
HA	CT	NZ	50.0	109.47	HHY	NHY	OHY	60.0	105.0
CH2E	CH1E	NZ	30.0	112.0	NHY	OHY	CH3E	60.0	109.0
CH1E	CH1E	NZ	30.0	112.0	NHY	OHY	CH2E	60.0	109.0
CH3E	CH1E	NZ	30.0	112.0	NHY	OHY	CH1E	60.0	109.0
CT	CT	NZ	30.0	112.0 ^d	NHY	OHY	CT	60.0	109.0 ^d
CH3E	NHY	OHY	80.0	105.0	NHY	OHY	C	60.0	115.0
CH1E	NHY	OHY	90.0	104.0	OHY	NHY	C	60.0	113.0
CH2E	NHY	OHY	80.0	105.0	OHY	CH2E	CH1E	60.0	104.0
CT	NHY	OHY	80.0	105.0	OHY	CH1E	CH2E	60.0	104.0
CH3E	NHY	CH3E	45.0	109.47	OHY	CT	CT	60.0	104.0 ^d
CH1E	NHY	CH1E	98.0	111.0	OE	CH1E	NHY	80.0	109.47
CH1E	NHY	CH2E	98.0	111.0	OE	CT	NHY	80.0	109.47
CT	NHY	CH2E	98.0	111.0	NHY	CH2E	C6R	70.0	114.0
CH1E	NHY	CH3E	70.0	109.0	NHY	CT	C6R	70.0	114.0 ^d
CT	NHY	CT	81.8	110.3 ^d	OHY	C	O	80.0	115.0
CH1E	NHY	C	77.5	116.0	OHY	C	CH3E	60.0	115.0
CT	NHY	C	77.5	116.0 ^d	OHY	C	CT	60.0	115.0 ^d
CH3E	C	NHY	110.0	116.0	OHY	CH1E	CUA1	80.0	109.47
CT	C	NHY	110.0	116.0 ^d	OHY	CT	CUA1	80.0	109.47 ^d
CH2E	CH1E	NHY	30.0	112.0	CH2E	CH1E	CUA1	45.0	100.0
CH1E	CH1E	NHY	90.0	110.0	NHY	CH1E	CUA1	70.0	111.6
CH3E	CH1E	NHY	30.0	112.0	NHY	CT	CUA1	70.0	111.6 ^d
CH1E	CT	NHY	30.0	112.0	OC	SO2	OC	144.0	120.0
CH1E	CH2E	NHY	30.0	109.0	C6R	SO2	OC	69.0	109.0
CT	CT	NHY	42.0	111.0 ^d	NT	SO2	OC	75.0	107.5
C6R	NHY	OHY	70.0	110.0	OE	CH1E	NX	70.0	113.0
C6R	C6R	NHY	90.0	120.0	OE	CT	NX	70.0	113.0 ^d
C6R	NHY	CH1E	70.0	115.0	NX	CH1E	NHY	65.0	104.0
C6R	NHY	CT	70.0	115.0 ^d	NX	CT	NHY	65.0	104.0 ^d
HA	CT	NHY	50.0	109.47	NX	C	NP	80.0	115.0
HA	CT	OHY	44.0	109.47					

^a In kcal.mol⁻¹. ^b In Å. ^c In kcal.mol⁻¹.Å⁻². ^d Average value. ^e In kcal.mol⁻¹.rad⁻². ^f In °. ^g In kcal.mol⁻¹.

results were treated with Unimap[®]* to give a 3D conformational map (Fig. 2). The map contained two areas of generally low energy, which corresponded to the conformers in which the N–O bond lies inside the sugar ring ($0^\circ < \varphi_1 < 120^\circ$), and to those for which φ_2 is close to 300° , *i.e.*, with N–O and H-2'–C-2' antiparallel, allowing easy rotation about the C-2–N bond. These two areas delimited a zone of high energy, the maxima of which corresponded to values of φ_2 close to either 120 or 240° . If the variation of energy *versus* φ_2 roughly presented a phase of $2\pi/3$, no such regular trend could be observed for φ_1 , the favourable values of which were 10 , 90 , 340 , and to a lesser extent 230° .

* A Trademark of UNIRAS A/S.

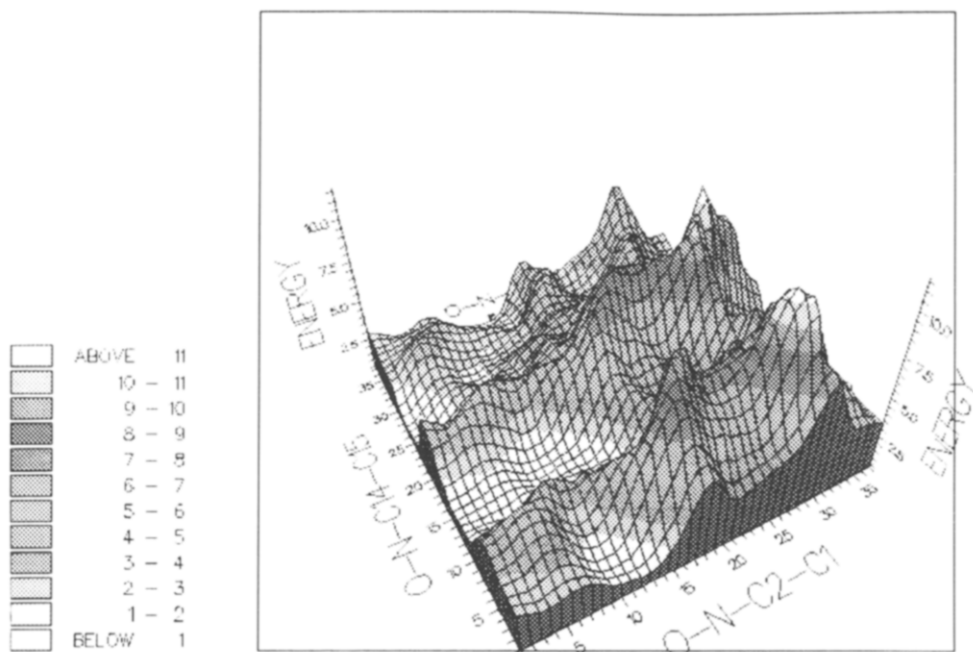


Fig. 2. Plot of CHARMm energy (kcal.mol^{-1}) versus φ_1 (O-N-C2-C1) and φ_2 (O-N-C14-C15) viewed from the origin ($\varphi_1 = \varphi_2 = 0^\circ$).

The area of lowest energy was centered at $\varphi_1 = 10^\circ$ and $\varphi_2 = 230^\circ$ (CHARMm energy, $0.34 \text{ kcal.mol}^{-1}$), extending to an adjoining area at φ_1 340 – 350° from which it was separated by a small energy barrier, and could correspond to conformer **5c** and to minimum A. A second area of low energy was centered at $\varphi_1 = 90^\circ$ and $\varphi_2 = 130^\circ$ (CHARMm energy, $0.59 \text{ kcal.mol}^{-1}$); it corresponded to a large, almost flat, surface (the conformer $\varphi_1 = 80^\circ$, $\varphi_2 = 130^\circ$ being only slightly less stable: CHARMm energy, $0.7 \text{ kcal.mol}^{-1}$; and the minimisation of a conformer $\varphi_1 = 76.6^\circ$ gave $\varphi_2 = 132^\circ$, with CHARMm energy, $0.63 \text{ kcal.mol}^{-1}$). This area could be associated with minimum B and approximated to conformer **6a**. A CHARMm energy barrier of 4 – 6 kcal.mol^{-1} between these two areas could be estimated (Fig. 2). The area of lowest possible energy, which could correspond to the minimum C found by AMPAC and to the conformer **6d**, was centered at $\varphi_1 = 230^\circ$ and $\varphi_2 = 330^\circ$, and was higher in energy (CHARMm energy, $1.6 \text{ kcal.mol}^{-1}$) than the two former minima and was extremely restricted in its possible values of φ_1 and φ_2 .

The results provided by quantum and molecular mechanics were in good overall semi-quantitative agreement with the experimental data and established with a reasonable reliability that the nitroxyl **3** exists as a mixture of one almost eclipsed conformer **5c** and an almost staggered conformer **6a**. Both computational techniques seemed to favour somewhat exaggerated, pure staggered conformers when the experimental values indicated a compromise between an eclipsed and a staggered form.

Even when dealing with frozen conformers, one experimental hyperfine coupling value associated with one torsional angle can correspond to one or more conformers out of a set of four, and neither chemical intuition nor use of mechanical molecular models easily permits the correct assignments. The situation is much more elaborate and confusing when dealing with time-averaged spectra.

Molecular mechanics, with parameters improved by fitting to more experimental data, may constitute a powerful and economical way to predict the conformation of sugar nitroxyls.

EXPERIMENTAL

The techniques used for e.s.r. measurements have been described¹⁹. The home-developed program used to simulate the e.s.r. spectra has been adapted to an IBM PC and its possibilities extended to the simulation of time-dependent processes.

Quantum and molecular mechanics computations as well as graphical representations were performed on a Silicon Graphics IRIS 4D70GT workstation.

ACKNOWLEDGMENTS

This work was supported by the Swiss National Research Foundation (grant No 20-26460-89). We thank M. P. Lichtle for his contribution to the development of the e.s.r. simulation program.

REFERENCES

- 1 J. M. J. Tronchet, N. Bizzozero, G. Bernardinelli, and M. Geoffroy, *Carbohydr. Res.*, 200 (1990) 469-474; J. M. J. Tronchet, R. Benhamza, G. Bernardinelli, and M. Geoffroy, *Tetrahedron Lett.*, 31 (1990) 531-534; J. M. J. Tronchet, R. Benhamza, N. Dolatshahi, M. Geoffroy, and H. Tuerler, *Nucleosides Nucleotides*, 7 (1988) 249-269.
- 2 J. M. J. Tronchet, G. Zosimo-Landolfo, N. Bizzozero, D. Cabrini, F. Habashi, E. Jean, and M. Geoffroy, *J. Carbohydr. Chem.*, 7 (1988) 169-186.
- 3 M. D. Wittman, R. L. Halcomb, and S. J. Danishefsky, *J. Org. Chem.*, 55 (1990) 1981-1983.
- 4 J. M. J. Tronchet, N. Bizzozero, M. Koufaki, F. Habashi, and M. Geoffroy, *J. Chem. Res. (S)*, (1989) 334; (*M*), 2601-2609.
- 5 J. M. J. Tronchet, N. Bizzozero, and M. Geoffroy, *Carbohydr. Res.*, 191 (1989) 138-143.
- 6 J. M. J. Tronchet, N. Bizzozero, M. Zsély, F. Barbalat-Rey, N. Dolashahi, G. Bernardinelli, and M. Geoffroy, *Carbohydr. Res.*, 212 (1991) 65-76.
- 7 A. Rassat and H. Lemaire, *J. Chim. Phys. Phys-Chim Biol.*, 61 (1964) 1576-1579; A. Rassat, H. Lemaire, and R. Ramasseul, *Mol. Phys.*, 8 (1964) 557-560.
- 8 J. M. J. Tronchet and S. Zerelli, *J. Carbohydr. Chem.*, 8 (1989) 217-232.
- 9 H. S. Gutowski and C. H. J. Holm, *J. Chem. Phys.*, 25 (1956) 1228-1234.
- 10 H. Eyring and M. Polanyi, *Z. Phys. Chem., Abt. B*, 11-12 (1931) 279-311.
- 11 QCPE program no 527.
- 12 T. Clark, SCAMP ver. 4.2, not published.
- 13 M. J. S. Dewar, E. G. Zoebisch, E. F. Healy, and J. J. P. Stewart, *J. Am. Chem. Soc.*, 107 (1985) 3902-3909.
- 14 QCPE program no 455, manual p 65.
- 15 B. R. Brooks, R. E. Bruccoleri, B. D. Olafson, D. J. States, S. Swaminathan, and M. Karplus, *J. Comput. Chem.*, 4 (1983) 187-217.

- 16 S. J. Weiner, P. A. Kollman, D. A. Case, U. C. Singh, C. Ghio, G. Alagona, S. Profeta, and P. J. Weiner, *J. Am. Chem. Soc.*, 106 (1984) 765–784; S. J. Weiner, P. A. Kollman, D. T. Nguyen, and D. A. Case, *J. Comput. Chem.*, 7 (1986) 230–242.
- 17 D. A. C. Compton, C. Chatgililoglu, H. H. Mantsch, K. V. Ingold, *J. Phys. Chem.*, 85 (1981) 3093–3100.
- 18 M.-M. Rohner, *J. Am. Chem. Soc.*, 113 (1990) 2875–2881.
- 19 J. M. J. Tronchet, E. Winter-Mihaly, J. Rupp, F. Barbalat-Rey, and M. Geoffroy, *Carbohydr. Res.*, 136 (1985) 375–390.